Quenching of the $3p\ ^4S^o$ atomic-nitrogen state in a low-pressure nitrogen glow discharge

A. Catherinot and A. Sy

Groupe de Recherche sur l'Energétique des Milieux Ionisés, Unité d'Enseignement et de Recherche de Sciences Fondamentales et Appliquées,

Université d'Orleans, 45045 Orleans Cedex, France

(Received 23 May 1979)

A laser perturbation method is used to determine the relaxation rate of the $3p\ ^4S^o$ state of atomic nitrogen as function of pressure and current intensity in a glow discharge. Quenching is due to spontaneous radiative transitions towards lower levels and to inelastic collisions with N_2 in the vibrationally excited ground state with a thermally averaged cross section of about 7.5×10^{-14} cm^2. Measurements allow the determination of the dissociation rate as a function of electronic temperature in the range 1–3 eV.

I. INTRODUCTION

In spite of the considerable amount of work devoted to collisional energy transfer between nitrogen atoms and molecules (See Refs. 1–4 and references therein), the collisional destruction of atomic nitrogen is not actually well understood. Reported studies, generally performed in high-frequency discharges, afterglows, or shock-heated plasmas, involve only atomic nitrogen in ground (^4S) and metastable (^2D, ^2P) states though results on collisional destruction of atomic excited states are of primary importance for a more detailed description of nitrogen plasmas by collisional-radiative models.[5,6]

In the present work quenching mechanisms of the $3p\ ^4S^\circ$ atomic nitrogen state are investigated by a time-resolved spectroscropic analysis of the population relaxations following a short resonant laser pulse pumping in a low-pressure glow discharge. Measurements performed for various experimental situations lead to the determination of the dissociation rate in the discharge and of the deexcitation channels of the $3p\ ^4S^\circ$ atomic state by collision with nitrogen molecules.

II. EXPERIMENT

The experimental setup is schematically shown in Fig. 1 and its essential details have been described in previous papers dealing with radiative and collisional processes in helium,[7] argon,[8] and hydrogen[9] glow discharges. A tunable dye laser excited by a Société de Production et de Recherche Appliquée (SOPRA) pulsed nitrogen laser. (pulse width 4 ns, spectral width 0.2 Å, energy/pulse ~ 10 μJ, repetition rate 15 Hz) is used to induce a short and selective perturbation of the $3p\ ^4S^\circ$ atomic nitrogen state population by resonant optical pumping.

In order to enhance the population on atomic nitrogen excited states, current pulses (current intensity I adjustable from 0 to 1.5 A) are superimposed on the continuous discharge current ($i = 10$ mA). Heating of the medium is avoided by a suitable choice of the current pulse duration (~40 μs) and a low repetition rate (~15 Hz). The other characterisitics of the discharge are the same as in Ref. 9. Measurements of the electrical potential between electrodes are made to ascertain that the glow discharge regime holds on during current pulses in the studied pressure range ($0.1 < P_{\text{Torr}} < 1.5$). The laser pulse is synchronized on the current pulse (jitter < 10 ns) and the time delay can be adjusted from 0 to 100 μs. For delay times greater than 20 μs after the beginning of the current pulse, the discharge reaches a stationary equilibrium as verified by oscillographic observation of atomic and molecular radiative emission. The results presented here are obtained with a typical time delay of 30 μs.

For each experimental situation (P, I) the corresponding value of the electronic density n_e is measured by a microwave cavity perturbation method. Typical results are shown on Fig. 2. Values of the mean electronic energy E_e, just estimated in the frame of glow discharge theory,[10] are shown in Fig. 3 as a function of the pressure P. The gas temperature is measured by a thermocouple in contact with the discharge tube ($T_g = 320 \pm 5$ K). After spatial filtering the pump laser beam traverses the discharge tube and great care is taken to prevent stray laser-light diffusion. The fluorescence light emitted by a cross section of the positive column is observed in a perpendicular direction and imaged by a fused silica lens ($f = 180$ mm, magnification = 1) onto the slits of a 2.0 m SOPRA grating spectrometer (resolving power 200 000 in the second order) and then onto a RCA 7265 photomultiplier tube (rise time = 2 ns). Time dependence of the output signal is analyzed in the same way as described in Ref. 9, by a Princeton Applied Research Boxcar averager (PAR 162) giving a time resolution of 5 ns. Each relaxation

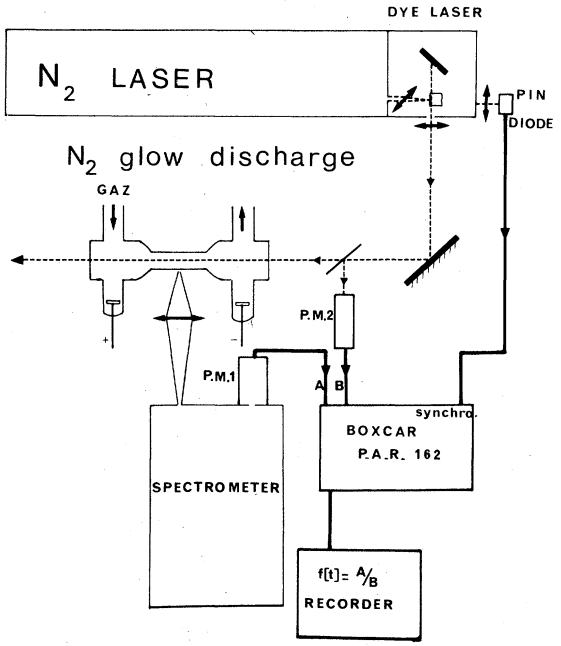

FIG. 1. Laser perturbation method experimental device.

curve corresponds to an average of 2×10^4 laser shots and great care is taken to avoid saturation of the electronic device by fluorescence light and saturation effects on the variations of the excited-state population.

III. MEASUREMENTS

A simplified diagram of atomic and molecular nitrogen energy states is shown in Fig. 4. Potential curves of N_2 are taken from Ref. 11 and atomic energy levels from Ref. 12. Variation of the $3p\,^4S^\circ(J=\frac{3}{2})$ NI (neutral atomic nitrogen) state population is induced by laser-optical pumping of the $2p^23s\,^4P(J=\frac{3}{2})$-$2p^23p\,^4S^\circ(J=\frac{3}{2})$ transition ($\lambda=7442.3$ Å; laser dye oxazine + R6G in ethanol) and studied for various discharge conditions (P, I). The relaxation $\Delta N(t)$ of the $3p\,^4S^\circ$ NI state population variation is deduced from measurements of the time variation of the spectrally integrated fluorescence light intensity at 7468 Å [$2p^23p\,^4S^\circ(J=\frac{3}{2})$-$2p^23S\,^4P(J=\frac{5}{2})$ radiative transition see Fig. 4 inset]. The laser spectral width well exceeds the width of the $\lambda=7442$ Å NI line emitted by the discharge, so the whole atomic velocity distribution is pumped.

Typical experimental results are shown in Fig. 5. After the laser has ceased the level population goes back to its equilibrium value with a quasi-exponential time dependence in all cases under study. Therefore, in this laser-free relaxation mode, the relaxation law of the $3p\,^4S^\circ$ level population variation is:

$$\Delta N(t)=\Delta N^\circ\exp(-\Gamma(P,I)t), \tag{1}$$

where $\Gamma(P,I)$ is the total quenching rate of the $3p\,^4S^\circ$ level and depends on the discharge pressure P and current intensity I. Typical values of $\Gamma(P,I)$ deduced from relaxation curves by Eq. (1) are shown in Fig. 6 as a function of P with I acting as a parameter. From these curves it follows, with a rather good approximation, that in present experimental conditions $\Gamma(P,I)$ can be expressed in the form

$$\Gamma(P,I)=A+B(I)P, \tag{2}$$

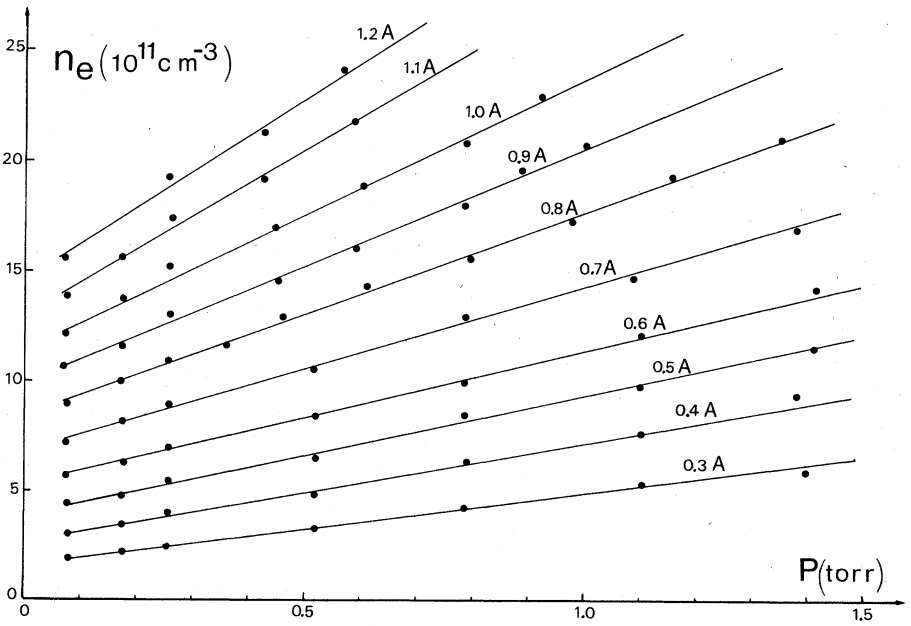

FIG. 2. Measured electronic density n_e as a function of the pressure P, current pulse intensity I acting as a parameter in the discharge.

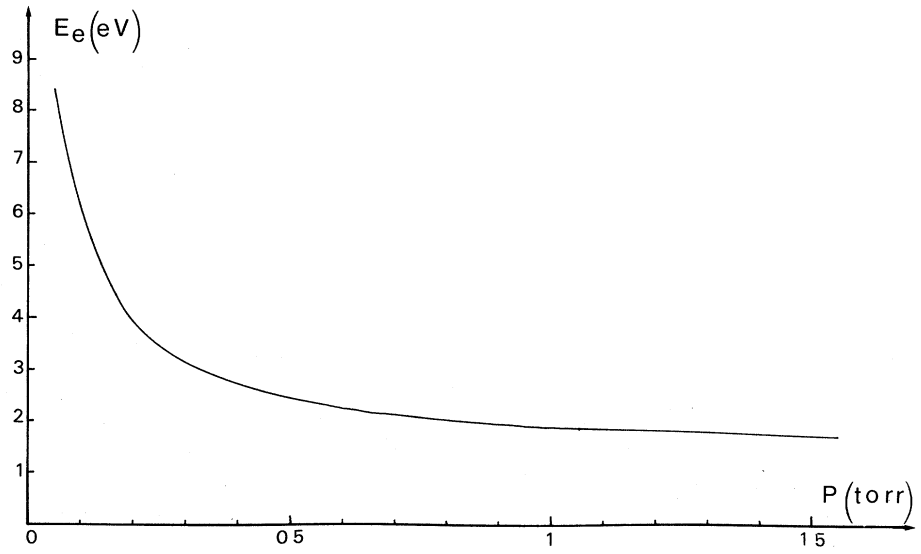

FIG. 3. Mean electronic energy E_e in the discharge as a function of the pressure P.

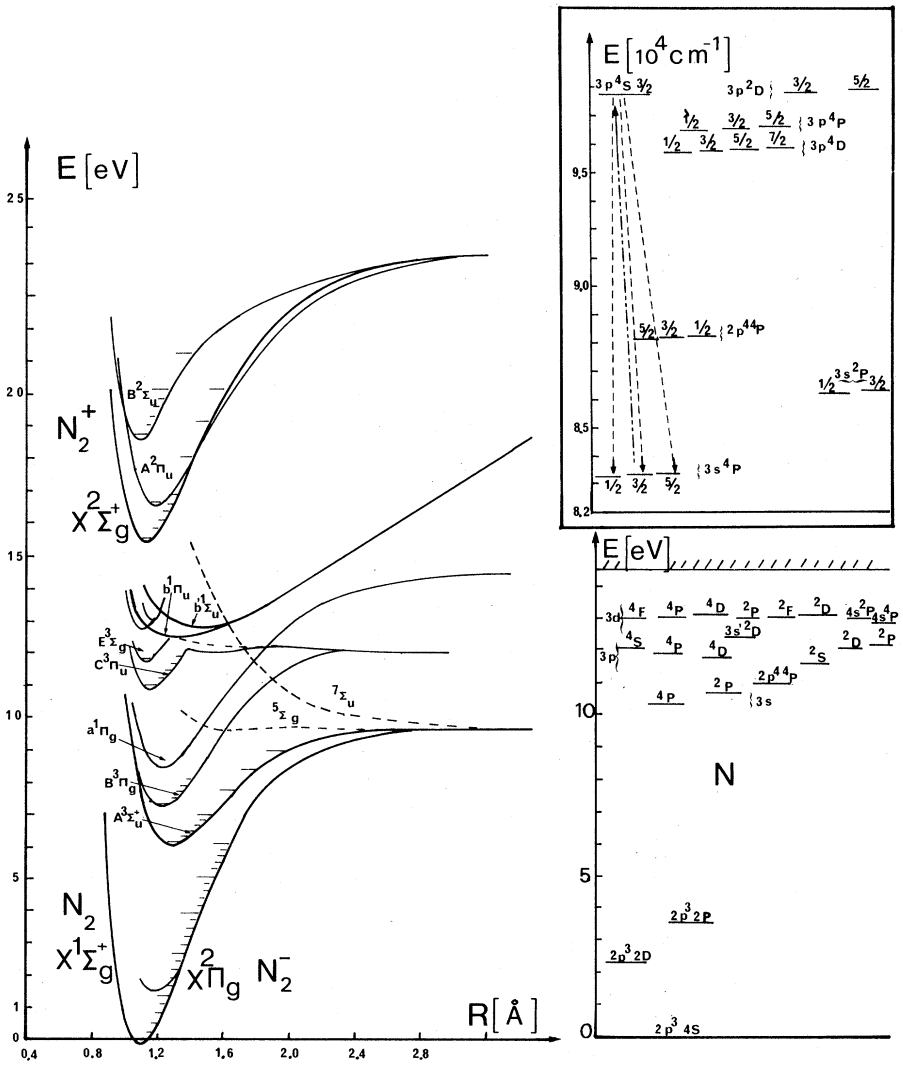

FIG. 4. Simplified diagram of nitrogen atomic and molecular energy states from Refs. 11 and 12. Inset: detail diagram of the $3p$ energy level of NI; (— ••— ••—) pumped transition 7442 Å.

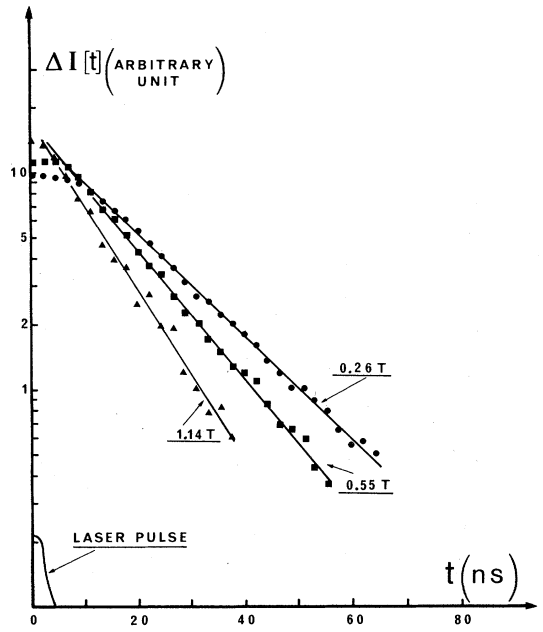

FIG. 5. Relaxation curves of the fluorescence light emitted from the $3p\,^4S^o$ NI state for a pulsed current intensity $I=1$ A and for pressures $P=0.26$ Torr (●), $P=0.55$ Torr (■), $P=1.14$ Torr (▲).

where A is a constant that does not depend on the pressure P and B is a function of I alone.

IV. INTERPRETATION

Generally, in a low-pressure nitrogen gas discharge, the quenching rate $\Gamma_n(P, I)$ of an excited atomic level $|n\rangle$ can be expanded as follows:

$$\Gamma_n(P,I) = \sum_{n'<n} A_{nn'}\Lambda_{nn'} + \sum_{n'\neq n}\sum_{\nu} n_{N_2}^{\nu} R_{\nu}^{nn'} + n_e \sum_{n'\neq n} S_{nn'} + n_N \sum T_{nn'} \,. \tag{3}$$

In this expression n_{N_2}, n_N, and n_e are, respectively, the molecular, atomic, and electronic population densities; $A_{nn'}$ and $\Lambda_{nn'}$ represent, respectively, the Einstein coefficient and the optical escape factor for the $|n\rangle \rightarrow |n'\rangle$ radiative transition; $R_{\nu}^{nn'}$, where ν describes a molecular state ($\nu=\Omega$, v, J) is the rate coefficient for the reaction

$$\mathrm{N}(|n\rangle) + \mathrm{N}_2(\nu) \rightarrow \mathrm{N}(|n'\rangle) + \mathrm{N}_2(\nu'); \tag{4}$$

$S_{nn'}$ is the excitation transfer-rate coefficient from state $|n\rangle$ towards state $|n'\rangle$ by electronic collisions

$$\mathrm{N}(|n\rangle) + \bar{e} \rightarrow \mathrm{N}(|n'\rangle) + \bar{e}; \tag{5}$$

and $T_{nn'}$ is the rate coefficient for the reaction

$$\mathrm{N}(|n\rangle) + \mathrm{N}(|g\rangle) \rightarrow \mathrm{N}(|n'\rangle) + \mathrm{N}(|g\rangle), \tag{6}$$

where $\mathrm{N}(|g\rangle)$ is the nitrogen atom in the ground state. Three-body collisions are neglected owing to their relatively low rate in the pressure range under study, and associative ionization is not possible due to a too large energy gap.

Under present experimental conditions no induced fluorescence light emitted in the lines originating from the $3p\,^2P^\circ$, $^2D^\circ$, $^4P^\circ$, and $^4D^\circ$ levels (see Fig. 4 inset) is observed when the $3p\,^4S^\circ$ level is overpopulated by laser-optical pumping. Consequently, excitation transfers by electronic, atomic, and molecular collisions, according to reactions

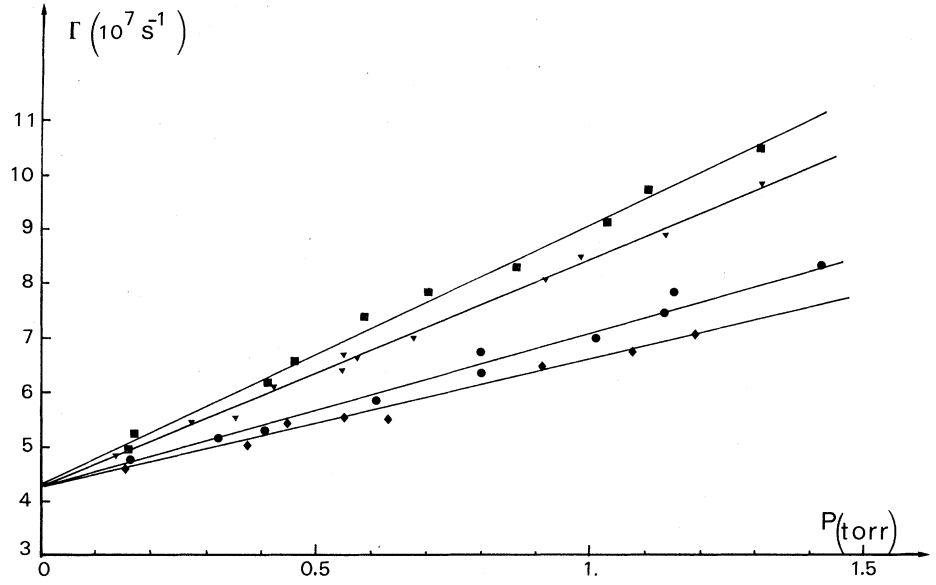

FIG. 6. Variations of the $3p\,^4S^o$ level quenching rate with pressure P for pulsed current intensities: $I=0.5$ A (♦), $I=0,6$ A (●), $I=1$ A (▼), and $I=1.3$ A (■).

TABLE I. Comparison of the measured total radiative destruction rate of the $3p\,^4S^o$ NI level with accepted values.

	Reference 13	Reference 14	Reference 6	This work
$\sum_{n'} A_{nn'}$ (10^8 s^{-1})	0.36 (25%)	0.433	0.440	0.43 (10%)

(4), (5) and (6), from the $3p\,^4S^\circ$ level towards nearby atomic energy levels are negligibly small. Therefore, one can write Eq. (3) in the approximate form

$$\Gamma(P,I)=\sum_{n'<n} A_{nn'}\Lambda_{nn'}+\sum_{\nu}\sum_{n'\neq n} n^{\nu}_{N_2}R^{nn'}_{\nu}\ , \tag{7}$$

where the last summation is performed on atomic levels $|n'\rangle$ excluding the $3p$ levels.

Comparison of Eq. (7) with Eq. (2) leads to:

$$A=\sum_{n'<n} A_{nn'}\Lambda_{nn'}\ B(I)P=\sum_{\nu}\sum_{n'\neq n} n^{\nu}_{N_2}R^{nn'}_{\nu}\ . \tag{8}$$

Then $B(I)P$ represents the total destruction rate by collisions with N_2 molecules and A appears as the total radiative decay rate.

Under the reasonable assumption of an optically thin medium ($\Lambda_{nn'}=1$) for radiative transition originating from the $3p\,^4S^\circ$ level (i.e., $3p\,^4S^\circ \rightarrow 3s\,^4P$ and $3p\,^4S^\circ \rightarrow 2s2p^4$), comparison can be done between measured and accepted values of A. As shown in Table I, a rather good agreement is obtained with calculated[13,14] and measured[6] values.

The values of $\Gamma(P,\ n_e)$ deduced from Figs. 6 and 2 are plotted in Fig. 7 as function of the electronic density n_e for three values of the pressure P. It follows from Eq. (6) that the observed variations of $\Gamma(P,\ n_e)$ can only be explained in terms of the variations of molecular population densities $n^{\nu}_{N_2}$, that is, by the variations of excitation and dissociation rates of molecular nitrogen with the electronic density n_e in the discharge. $\Gamma(P,\ n_e)$ exhibits a quasilinear dependence on n_e for $n_e \lesssim 1.2\times10^{12}$ cm^{-3} followed by a saturation for larger n_e values. An extrapolation of these quasilinear parts to zero electronic density leads to values of $\Gamma(P,\ n_e=0)$ which do not depend on the pressure P and which are equal to the measured total radiative deexcitation probability A of the $3p\,^4S^\circ$ level, at measurement accuracy. Thus, in our experimental conditions, only collisions involving excited molecular states, the population of which depends on n_e, are efficient collisional quenching mechanisms of the $3p\,^4S^\circ$ atomic nitrogen state. The contribution of the reaction

$$N(3p\,^4S^\circ)+N_2(X^1\Sigma^+_g,\ v=0,J)\rightarrow N+N^*_2$$

is then negligibly small.

A tentative interpretation of the experimental results can be made within the framework of the following elementary model. First, we assume that in the low-pressure nitrogen glow discharge an excited molecular state ν is mainly produced by the reaction

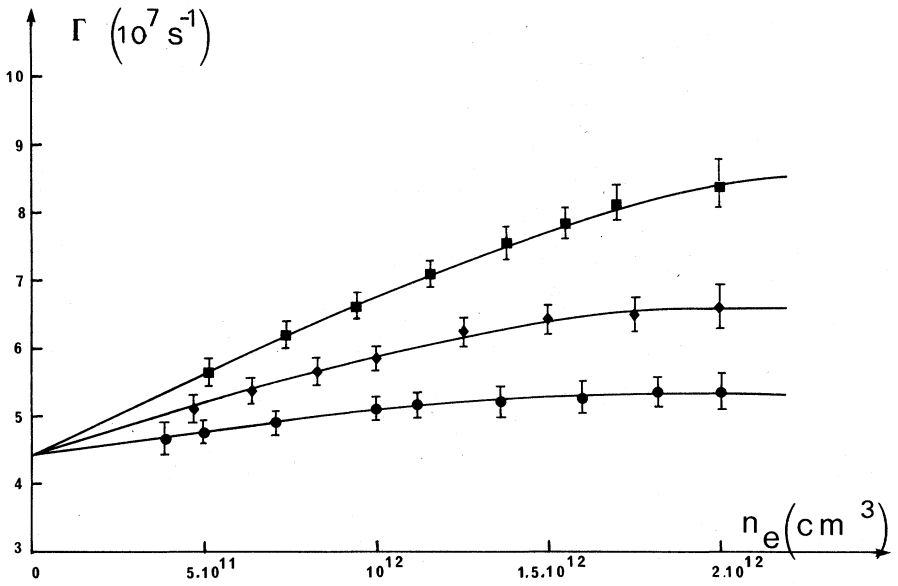

FIG. 7. Variations of the $3p\,^4S^o$ level quenching rate with n_e for pressure P = 1 Torr (■), P = 0,5 Torr (♦), and P = 0,25 Torr (●). Continuous curves: fit of experimental results by Eq. (17).

$$N_2(X^1\Sigma_g^+, v=0, J)+\bar{e}\rightarrow N_2(v)+\bar{e}. \quad (9)$$

The population density $n_{N_2}^v$ is then described by the rate equation

$$\frac{dn_{N_2}^v}{dt}=n_{N_2}^X n_e Q^v - n_{N_2}^v T^v, \quad (10)$$

where Q^v is the rate coefficient for reaction (9) and T^v is the total destruction coefficient of the $N_2(v)$ state. In quasistationary equilibrium one has

$$n_{N_2}^v = n_{N_2}^X n_e Q^v/T^v. \quad (11)$$

Secondly, assuming that the reaction

$$N_2(X)+\bar{e}\rightarrow N+N+\bar{e} \quad (12)$$

is mainly responsible for dissociation processes in the discharge, the number density n_N of atomic nitrogen is described by the rate equation

$$\frac{dn_N}{dt}=2n_{N_2}n_e F - n_N R, \quad (13)$$

where F is the rate coefficient for reaction (12) and R is the total destruction-rate coefficient of atomic nitrogen. In a quasistationary equilibrium one has

$$n_N = n_{N_2} n_e 2F/R. \quad (14)$$

Now, at constant pressure P we have

$$n_{N_2}=n_{N_2}^\circ - n_N, \quad (15)$$

where $n_{N_2}^\circ = P/kT_g$ is the molecular population density at total pressure P and gas temperature T_g without any dissociation, that is, without discharge. Then, for given values of P and I, we obtain

$$n_{N_2}^v = (P/kT_g)(Q^v/T^v)[n_e/(1+n_e 2F/R)]. \quad (16)$$

Comparison with Eq. (8) leads to

$$B(I)=(K/kT_g)\,[n_e/(1+n_e C)], \quad (17)$$

where

$$K=\sum_{\substack{n'\neq n\\ v}} \frac{Q^v}{T^v} R_v^{nn'} \quad (18)$$

and

$$C = 2F/R. \quad (19)$$

Here the gas temperature is constant and consequently C depends only on the electronic mean kinetic energy E_e, that is, on the pressure P since in glow discharge E_e is only a function of pressure P and tube diameter.[10] On the other hand, K generally depends on E_e, T_g, and vibrational temperature T_v.

The coefficients K and C, the latter characterising the dissociation in the discharge, are obtained through comparison of experimental curves Fig. 7 with Eq. (17) by a least-squares procedure for various experimental situations. Some results of the fitting procedure are plotted on Fig. 7 and exhibit a very good agreement with measurements. Corresponding calculated values of the coefficients K and C are shown on Fig. 8 as functions of the mean electronic kinetic energy E_e deduce from Fig. 3.

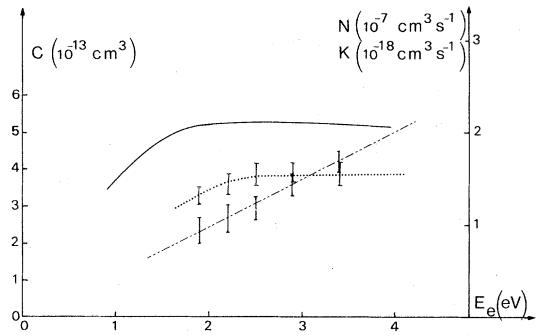

FIG. 8. Values of coefficients K (•••) and C (••—••) [Eqs. (18) and (19)] as functions of the mean-electronic kinetic energy E_e; continuous curve: "effective electron vibrational excitation rate" after Ref. 22.

V. DISCUSSION

A. Dissociation

As previously quoted dissociation and re-association processes in nitrogen plasma are not yet well understood. In previous works collisional $N-N_2$ mechanisms have been studied by means of various experimental methods. As examples, measurements of atomic nitrogen density have been performed in afterglow by NO (nitric oxide) titration techniques[2] and by the analysis of Lewis-Rayleigh afterglow decay[15]; the latter method has been used for the same purpose in shock heated $N-N_2$ mixture[1] whereas measurements of the molecular disappearance, using vacuum ultraviolet light absorption in shock tube are reported in Ref. 16. Unfortunately, a comparison with the presently measured coefficient C is not possible due to completely different plasma conditions. However, the dissociation rate coefficient F [reaction (12)] can be estimated by integration on a Maxwellian electronic velocity distribution of the dissociation cross sections of molecular nitrogen measured by Winters[17] and Rapp *et al.*[18] Then the destruction coefficient R of atomic nitrogen in the discharge can be calculated by Eq. (19). As shown on Fig. 9, R depends linearly on $1/P$, that is it depends linearly on the mean free path in the discharge. This fact expresses clearly the well-known result that, in a capillary low-pressure nitrogen glow discharge, atom disappearance is mainly due to

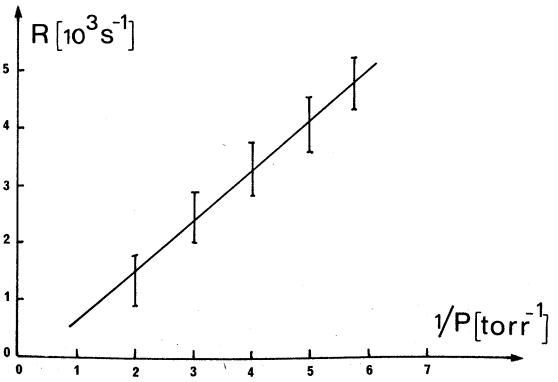

FIG. 9. Destruction coefficient R of atomic nitrogen as a function of $1/P$.

diffusion and recombination on the discharge walls[15] and confirms the assumption that reaction (12) is the dominant process for dissociation in our experiment.

B. Destruction of the $3p\,^4S^o$ atomic state

As shown previously, the $3p\,^4S^\circ$ state collisional destruction is mainly due to collisions with molecular nitrogen in excited states. The efficiency of the collisional quenching mechanism suggests that the molecular states responsible for this quenching effect must be sufficiently populated metastable ones, that is, $A\,^3\Sigma_u^+$ in a low vibrational state or a vibrationally excited $X\,^1\Sigma_u^+$ ground state. Furthermore, the reaction must be energetically quasiresonant ($\Delta E < kT_g$).

In order to determine the collisional deexcitation channels of the $3p\,^4S^\circ$ atomic state we have systematically investigated the reactions

$$\mathrm{N}(3p\,^4\mathrm{S}^\circ) + \mathrm{N}_2(v) \rightarrow \mathrm{N}(|n'\rangle) + \mathrm{N}_2(v') + \Delta E\,, \qquad (20)$$

provided they are energetically quasiresonant (i.e., $|\Delta E| \lesssim kT_g$) and consistent with Wigner spin conservation rules in the collision. Among the numerous possible reactions the most probable correspond to dipole-allowed transitions in the molecule and in the atom.

When v in reaction (20) is supposed to be a low vibrationally excited $A\,^3\Sigma_u^+$ state, investigation of

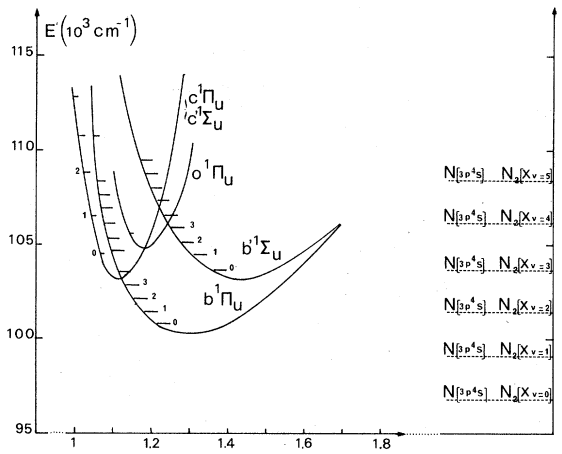

FIG. 10. Partial energy diagram of the $b\,^1\Pi_u$ and $b'\,^1\Sigma_u^+$ valence states and of the $c_n\,^1\Pi_u$, $c_n'\,^1\Sigma_u^+$ and $o\,^1\Pi$ Rydberg states: possible deexcitation channels of the $3p\,^4S^o$ atomic state according to reactions (23)–(26) (see text).

spectroscopic data tables[19] indicates that the most propitious situations arise for the reactions

$$\mathrm{N}(3p\,^4\mathrm{S}^\circ) + \mathrm{N}_2(A\,^3\Sigma_u^+, v=2) \rightarrow \mathrm{N}(3s\,^4P) + \mathrm{N}_2(B\,^3\pi_g, v=4) + \Delta E \quad (\Delta E \simeq 65\ \mathrm{cm}^{-1}) \qquad (21)$$

and

$$N(3p\,^4S^o) + \mathrm{N}_2(A\,^3\Sigma_u^+, v=3) \rightarrow N(3s\,^4P) + \mathrm{N}_2(B\,^3\pi_g, v=5) + \Delta E \quad (\Delta E \simeq -150\ \mathrm{cm}^{-1}). \qquad (22)$$

Despite quasiresonant situations and dipole-allowed transitions, no induced fluorescence light is observed originating from the $(B\,^3\pi_g, v=4)$ and $(B\,^3\pi_g, v=5)$ states. Thus the contribution of the $A\,^3\Sigma_u^+$ metastable state to the destruction of the $3p\,^4S^\circ$ state may be considered as negligibly small.

When v in reaction (20) is supposed to be a vibrationally excited state of the $X\,^1\Sigma_g^+$ molecular ground state, investigation of spectroscopic data[19,20] indicates that quasiresonant situations occur for the reactions (see Fig. 10):

$$N(3p\,^4S^\circ) + \mathrm{N}_2(X\,^1\Sigma_g^+, v=2) \rightarrow \mathrm{N}(2p^3\,^4S^\circ) + \mathrm{N}_2(b\,^1\pi_u, v=1) + \Delta E \quad (\Delta E \simeq -20\ \mathrm{cm}^{-1}) \qquad (23)$$

$$\mathrm{N}(3p\,^4\mathrm{S}^\circ) + \mathrm{N}_2(X\,^1\Sigma_g^+, v=3) \rightarrow \mathrm{N}(2p^3\,^4\mathrm{S}^\circ) + \mathrm{N}_2(b\,^1\pi_u, v=4) + \Delta E \quad (\Delta E \simeq +200\ \mathrm{cm}^{-1}) \qquad (24)$$

$$\mathrm{N}(3p\,^4\mathrm{S}^\circ) + \mathrm{N}_2(X\,^1\Sigma_g^+, v=3) \rightarrow \mathrm{N}(2p^3\,^4\mathrm{S}^\circ) + \mathrm{N}_2(b'\,^1\Sigma_u^+, v=0) + \Delta E \quad (\Delta E \simeq +100\ \mathrm{cm}^{-1}) \qquad (25)$$

$$\mathrm{N}(3p\,^4\mathrm{S}^\circ) + \mathrm{N}_2(X\,^1\Sigma_g, v>3) \rightarrow \mathrm{N}(2p^3\,^4\mathrm{S}^\circ) + \mathrm{N}_2 \begin{cases} b\,^1\pi_u, & v>4 \\ b'\,^1\Sigma_u^+, & v>0 \\ c_n\,^1\pi_u \\ c_n'\,^1\Sigma_u^+ \\ o\,^1\pi_u \end{cases} \qquad (26)$$

Among this great number of collisional deexcitation channels of the $3p\,^4S^\circ$ atomic state the most efficient is probably reaction (23) owing to the large number of molecules in the $(X\,^1\Sigma_g^+,\ v=2)$ state, quasiresonant situation ($\Delta E \sim -20$ cm^{-1}), and transition in agreement with the Franck-Condon principle.

From the above discussion it appears that the main collisional quenching mechanisms of the $3p\,^4S^o$ atomic state is in all probability

$$N(3p\,^4S^\circ) + N_2(X\,^1\Sigma_g^+,\ v \geq 2) \rightarrow N(2p^3\,^4S^\circ) + N_2 \begin{cases} b\,^1\pi_u \\ b'\,^1\Sigma_u^+ \\ c_n\,^1\pi_u \\ c_n'\,^1\Sigma_u^+ \\ o\,^1\pi_u \end{cases}; \tag{27}$$

then the coefficient K [Eq. (18)] may be written

$$K = \sum_{v\geq 2} \left(\frac{Q(X,v)}{T(X,v)}\right) R(X,v) \tag{28}$$

and the total destruction rate becomes

$$\Gamma = A + n_{N_2(X\,^1\Sigma_g^+,\ v\geq 2)} k\,. \tag{29}$$

In Eq. (28) $Q(X,\ v\geq 2)$ depends on E_e, $T(X, v\geq 2)$ is a function of the "vibrational temperature of the $X\,^1\Sigma_g^+$ state" T_v [in a low-pressure nitrogen gas discharge, the main destruction mechanism of a vibrational excited state is V.V. (vibration-vibration) exchange[21,22]], and $R(X,v)$ depends only on the gas temperature T_g.

A comparison is made in Fig. 8 between the measured K dependence on E_e and the variation of the "effective electron vibrational excitation rate" calculated by Nighan[22] in the 1–3 eV range typical of electrical discharge. A similar behavior is observed. This fact gives an important support to the assumption that reaction (27) is the main collisional destruction process of the $3p\,^4S^\circ$ atomic state.

In order to calculate the rate coefficient k by Eq. (29) an estimate of the population density in the $(X\,^1\Sigma_g^+,\ v\geq 2)$ molecular nitrogen states is necessary. The problem has been solved in the following way.[23] We assume that the $(C\,^3\pi_u, v)$ state is populated according to reaction (9) and that deexcitation of the $(C\,^3\pi_u,\ v)$ state is mainly due to spontaneous radiative transitions towards the $B\,^3\pi_g$ state. This fact is actually correct in low-pressure nitrogen discharge $P \lesssim 1$ Torr due to the short radiative lifetime of the $C\,^3\pi_u$ state (~ 40 ns). Under these assumptions the population density in the $(C\,^3\pi_u,\ v)$ state may be written in a quasistationnary state

$$n_{N_2}(C\,^3\Pi_u, v) = \frac{\sum_{v''} n_{N_2}(X\,^1\Sigma_g^+, v'')\, Q(X, v''; C, v)}{\sum_{v'} A(C, v; B, v')}, \tag{30}$$

where $Q(X,\ v'';\ C, v)$ is the rate coefficient for the reaction

$$N_2(X\,^1\Sigma_g^+, v'') + \bar{e} \rightarrow N_2(C\,^3\Pi_u, v) + \bar{e}$$

and $A(C, v;\ B, v')$ is the probability for the $(C\,^3\Pi_u,\ v) \rightarrow (B\,^3\Pi_g,\ v')$ spontaneous radiative transition.

Assuming next that $Q(X,\ v'';\ C,\ v)$ is proportional to the corresponding Franck-Condon factor $q(v'',\ v)$[24] and a Boltzmann distribution on vibrationally excited $X\,^1\Sigma_g^+$ states, we can write in a first approximation

$$\frac{n_{N_2}(C, v_1)}{n_{N_2}(C, v_2)} = \frac{\sum_{v''} q(v'', v_1) \exp(-Ev''/kT_g)}{\sum_{v''} q(v'', v_2) \exp(-Ev''/kT_g)} \times \frac{\sum_{v''} A(C, v_1; B, v')}{\sum_{v''} A(C, v_2; B, v')}, \tag{31}$$

where Ev'' is the energy of the $(X\,^1\Sigma_g^+,\ v'')$ vibrationally excited state. The ratios $n_{N_2(C,\,v_1=1)}/n_{N_2(C,\,v_2=0)}$ and $n_{N_2(C,\,v_1=2}/n_{N_2(C,\,v_2=0)}$ are deduced from measured integrated intensities of the $0\rightarrow 2$, $1\rightarrow 3$, and $2\rightarrow 4$ bands of the second positive system of N_2. Computed Franck-Condon factors of Benesch *et al.*[25] and radiative transition probabilities measured by Shemansky *et al.*[26] are used to calculate, by Eq. (31), the same ratios for given values of T_v. Comparison of both calculated and measured datas leads to an estimate of the "vibrational temperature" T_v in the $X\,^1\Sigma_g^+$ molecular nitrogen ground state, which is found to depend only slightly on pressure and discharge current intensity and lies at about 6000 K, in the ranges of interest.

Taking into account the dissociation and assuming a Boltzmann population distribution on the $X\,^1\Sigma_g^+$ vibrationally excited states at $T_v \sim 6000$ K, the population density on the $v\geq 2$ states is computed and by Eq. (29) the collisional quenching-rate coefficient k is deduced. Calculations performed for various experimental situations leads to

$$k = (6.5 \pm 2) \times 10^{-9}\ \text{cm}^3\,\text{s}^{-1}, \tag{32}$$

and the thermally averaged cross-section σ is found to be

$$\sigma = (7.5 \pm 2) \times 10^{-14}\ \text{cm}^2. \tag{33}$$

Unfortunately these values cannot be compared with previous works since to our knowledge no other published results on this subject exist at the present time. However, the value of σ is of the same order of magnitude as that of the previously

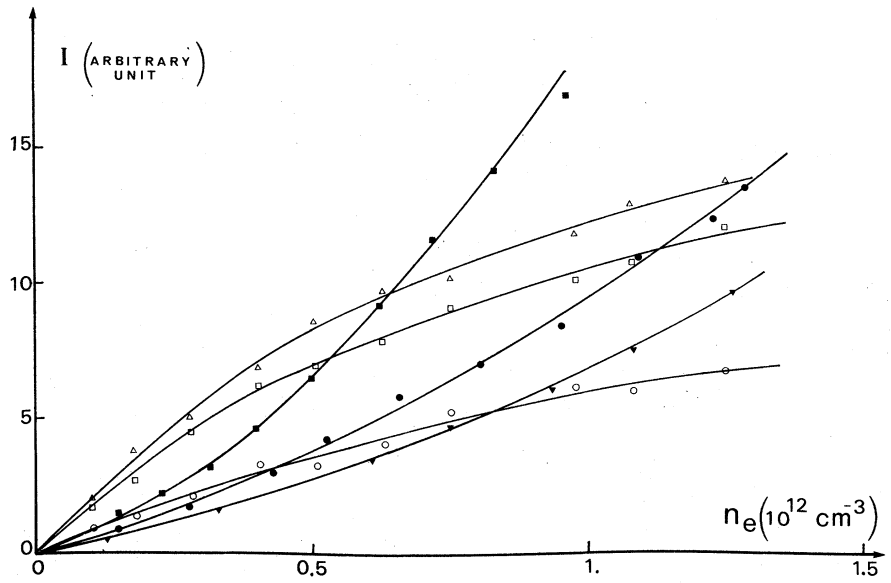

FIG. 11. Variations of the $\lambda = 7468$ Å NI line intensity for various pressure values $P = 0.31$ Torr (■), 0.85 Torr (●), and 1.13 Torr (▼) and variations of the $0 \rightarrow 2$ (△), $1 \rightarrow 3$ (□), and $2 \rightarrow 4$ (○) band intensities of the second positive system for $P = 1$ Torr as functions of the electronic density n_e.

measured destruction cross sections of atomic hydrogen $n = 3$, 4, 5 excited states by collision with quasimetastable $c\,^3\Pi_u$ and $a\,^3\Sigma_u^+$ states of H_2 in a hydrogen low-pressure glow discharge.[9]

C. Justification of the proposed model

In order to check the validity of the proposed model of molecular excitation and dissociation we have measured the variation of the atomic and molecular line intensities as functions of the pressure P and the current intensity I in the discharge. Some examples are shown in Fig. 11. We observe that the variations with the electronic density n_e of the $0 \rightarrow 2$, 1–3, and 2–4 band intensities of the second positive system are rather well described by Eq. (16). On the other hand, the $\lambda = 7468$ Å atomic line intensity depends quadratically on n_e, at least for $n_e < 1.5 \times 10^{12}$ cm^{-3}. Assuming that the $3p\,^4S^\circ$ excited atomic state is populated by direct electronic excitation according to the reaction

$$N(2p^3\,^4S^\circ) + \bar{e} \rightarrow N(3p\,^4S^\circ) + \bar{e}\,, \tag{34}$$

Eq. (14) gives for the $3p\,^4S^\circ$ state population density

$$n_{N(3p\,^4S^\circ)} \simeq n_e^2 S(E_e) n_{N_2} C(E_e)\,, \tag{35}$$

where $S(E_e)$ is the rate coefficient for reaction (34).

Then, at least for low dissociation rate, $n_{N(3p\,^4S^\circ)}$ just depends quadratically on the electronic density n_e, as experimentally found. The results confirm that the proposed model describes, at least roughly, excitation and dissociation in the discharge.

VI. CONCLUSION

We have measured by a laser perturbation method the total quenching rate of the $3p\,^4S^\circ$ atomic nitrogen state in a glow nitrogen discharge. Measurements performed for various experimental situations allow the determination of a "dissociation coefficient" and its variation with the mean electronic energy in the range 1–3 eV. On the other hand, the experimental results show that destruction of the $3p\,^4S^\circ$ state is due to spontaneous radiative transitions and collisions with vibrationally excited ground-state molecules. The most efficient collisional deexcitation channel is in all probability

$$N(3p\,^4S^\circ) + N_2(X\,^1\Sigma_g^+, v = 2) \rightarrow N(2p^3\,^4S^\circ) + N_2(b\,^1\Pi_u, v = 1)\,.$$

The large value obtained for the collisional quenching-rate coefficient may explain that in nitrogen plasmas, with relatively low dissociation rates, the atomic lines originating from levels $|n\rangle$ lying above ~ 101 000 cm^{-1} are completely quenched, whereas the lines originating from atomic levels lying under this "threshold" are fairly well observed. Indeed, assuming that the rate coefficient of reactions,

$$N(|n\rangle) + N_2(X\,^1\Sigma_g^+, v \geq 0) \rightarrow N + N_2 \begin{cases} b\,^1\Pi_u \\ b'\,^1\Sigma_u^+ \\ c_n\,^1\Pi_u \\ c_n'\,^1\Sigma_u^+ \\ o\,^1\Pi_u \end{cases},$$

is of the same order of magnitude as the one measured for the $3p\,^4S^\circ$ state, we obtain collisional lifetime of about 5 ns, very short compared to typical

radiative lifetimes of states $|n\rangle$. Moreover, due to the great number of excitation-transfer channels for the atomic states energetically lying above the previously defined "threshold," it is clear that their collisional quenching rates are much larger then the one we have measured for the $3p\,^4S^\circ$ state.

We consider that this "threshold" observed for the emission of atomic nitrogen lines make the $b\,^1\Pi_u$ and $b'\,^1\Sigma_u^+$ valence states and the $c_n\,^1\Pi_u$, $c_n'\,^1\Sigma_u^+$, and $o\,^1\Pi_u$ Rydberg molecular states good candidates for final products in quenching reactions of atomic excited states by collision with molecular nitrogen.

The thermally averaged cross section $\sigma = 7.5 \times 10^{-14}$ cm^2 indicates the great efficiency of the mechanisms which strongly connect the atomic and molecular states. This coupling through atom-molecule excitation transfer tends to depopulate the atomic excited states for the benefit of excited molecular states, leading to an apparent increase of N_2 rotational temperatures and an apparent decrease of the atomic excitation temperature as generally observed in low-pressure nitrogen glow discharges (Here $T_g \sim 320$ K, $T_R \sim 420$ K, atomic excitation temperature $T_{EX} \sim 2000$ K, and $T_e \sim 25\,000$ K).

ACKNOWLEDGMENTS

The technical assistance of M. Dudemaine for the electronic synchronization device design is gratefully acknowledged.

[1]K. Wray, J. Chem. Phys. 44, 623 (1964).
[2]I. M. Campbell and B. A. Thrush, Proc. R. Soc. A 296, 201 (1967).
[3]M. F. Golde and B. A. Thrush, Chem. Phys. Lett. 8, 375 (1971).
[4]K. H. Becker, W. Groth, and D. Kley; Z. Naturforsch. Teil A 24, 1840 (1969).
[5]A. Catherinot and A. Sy, Z. Naturforsch. Teil A 30, 1143 (1975).
[6]C. Park, J. Plasma Phys. 9, 187 (1973).
[7]B. Dubreuil and A. Catherinot, Physica C 93, 408 (1978). B. Dubreuil and A. Catherinot, J. Phys. D 11, 1043 (1978).
[8]A. Catherinot, P. Placidet, and B. Dubreuil, J. Phys. B 11, 3775 (1978).
[9]A. Catherinot, B. Dubreuil, and M. Gand, Phys. Rev. A 18, 1097 (1978). B. Dubreuil and A. Catherinot, J. Phys. (Paris) 39, 1071 (1978).
[10]S. C. Brown, *Basic Data of Plasma Physics* (Wiley, New York, 1959).
[11]F. Gilmore, J. Quant. Spectrosc. Radiat. Transfer 5, 369 (1965).
[12]C. Moore, *Atomic Energy Levels*, U. S. Natl. Bur. Stand. Circ. 467 (U.S. Dept. of Commerce, Washington, D. C., 1949), Vol. I.
[13]W. L. Wiese, M. W. Smith, and B. M. Glennon, Nat. Stand. Ref. Data Ser., Nat. Bur. Stand. 1, 4 (1966).
[14]H. R. Griem, *Plasma Spectroscopy* (McGraw-Hill, New York, 1964).
[15]R. E. Lund and H. J. Oskam, J. Chem. Phys. 48, 109 (1968).
[16]J. P. Appleton, M. Steinberg, and D. J. Liquornik, J. Chem. Phys. 48, 599 (1968).
[17]H. F. Winters, J. Chem. Phys. 44, 1472 (1966).
[18]D. Rapp, P. Englander-Golden, and D. D. Briglia, J. Chem. Phys. 42, 4081 (1965).
[19]B. Rosen, *Spectroscopic Data Relative to Diatomic Molecules* (Pergamon, Oxford, 1970); G. H. Dieke and D. F. Heath, *John Hopkins Spectroscopy Report No.* 17 (unpublished).
[20]P. K. Carrol and C. P. Collins, Can. J. Phys. 47, 563 (1969). K. Dressler, *ibid.* 47, 547 (1969). A. Lefebvre-Brion and C. M. Moser, J. Chem. Phys. 43, 1394 (1965); P. K. Carrol, C. P. Collins and K. Yoshino, J. Phys. B 3, L127 (1970); P. K. Carrol and K. Yoshino, *ibid.* 5, 1614 (1972).
[21]M. Capitelli and M. Dilonardo, Rev. Phys. Appl. 13, 115 (1978).
[22]W. L. Nighan, Phys. Rev. A 2, 1989 (1970).
[23]L. Hochard, A. Ricard, and M. Touzeau (unpublished).
[24]S. J. Young and K. L. Horn, J. Chem. Phys. 57, 4835 (1972).
[25]W. Benesh, J. T. Vanderlice, S. G. Tilford, and P. G. Wilkinson, Astrophys. J. 143, 236 (1966).
[26]D. E. Shemansky and A. L. Broadfoot, J. Quant. Spectrosc. Radiat. Transfer 11, 1385 (1971).